



This is a repository copy of *Estimating drag coefficient for arrays of rigid cylinders representing emergent vegetation*.

White Rose Research Online URL for this paper:
<http://eprints.whiterose.ac.uk/136433/>

Version: Published Version

Article:

Sonnenwald, F.C. orcid.org/0000-0002-2822-0406, Stovin, V. and Guymer, I. (2018)
Estimating drag coefficient for arrays of rigid cylinders representing emergent vegetation.
Journal of Hydraulic Research/De Recherches Hydrauliques. ISSN 0022-1686

<https://doi.org/10.1080/00221686.2018.1494050>

Reuse

This article is distributed under the terms of the Creative Commons Attribution (CC BY) licence. This licence allows you to distribute, remix, tweak, and build upon the work, even commercially, as long as you credit the authors for the original work. More information and the full terms of the licence here:
<https://creativecommons.org/licenses/>

Takedown

If you consider content in White Rose Research Online to be in breach of UK law, please notify us by emailing eprints@whiterose.ac.uk including the URL of the record and the reason for the withdrawal request.



eprints@whiterose.ac.uk
<https://eprints.whiterose.ac.uk/>



Estimating drag coefficient for arrays of rigid cylinders representing emergent vegetation

Fred Sonnenwald, Virginia Stovin & Ian Guymer

To cite this article: Fred Sonnenwald, Virginia Stovin & Ian Guymer (2018): Estimating drag coefficient for arrays of rigid cylinders representing emergent vegetation, Journal of Hydraulic Research, DOI: [10.1080/00221686.2018.1494050](https://doi.org/10.1080/00221686.2018.1494050)

To link to this article: <https://doi.org/10.1080/00221686.2018.1494050>



© 2018 The Author(s). Published by Informa UK Limited, trading as Taylor & Francis Group



Published online: 28 Sep 2018.



Submit your article to this journal [↗](#)



Article views: 107




View Crossmark data [↗](#)



Technical note


Estimating drag coefficient for arrays of rigid cylinders representing emergent vegetation

FRED SONNENWALD  (IAHR Member), *Research Associate, Department of Civil and Structural Engineering, University of Sheffield, Sheffield, UK*

Email: f.sonnenwald@sheffield.ac.uk (author for correspondence)

VIRGINIA STOVIN  , Reader in Urban Drainage, *Department of Civil and Structural Engineering, University of Sheffield, Sheffield, UK*

Email: v.stovin@sheffield.ac.uk

IAN GUYMER  (IAHR Member), *Professor of Civil Engineering, Department of Civil and Structural Engineering, University of Sheffield, Sheffield, UK*

Email: i.guymer@sheffield.ac.uk

ABSTRACT

Flow resistance due to vegetation is of interest for a wide variety of hydraulic engineering applications. This note evaluates several practical engineering functions for estimating bulk drag coefficient (C_D) for arrays of rigid cylinders, which are commonly used to represent emergent vegetation. Many of the evaluated functions are based on an Ergun-derived expression that relates C_D to two coefficients, describing viscous and inertial effects. A re-parametrization of the Ergun coefficients based on cylinder diameter (d) and solid volume fraction (ϕ) is presented. Estimates of C_D are compared to a range of experimental data from previous studies. All functions reasonably estimate C_D at low ϕ and high cylinder Reynolds numbers (R_d). At higher ϕ they typically underestimate C_D . Estimates of C_D utilizing the re-parametrization presented here match the experimental data better than estimates of C_D made using the other functions evaluated, particularly at low ϕ and low R_d .

Keywords: Cylinder arrays; drag coefficient; estimating drag; porous media; vegetated flows

1 Introduction

Vegetation occurs in many natural and engineered water systems (O'Hare, 2015). In rivers the additional drag caused by vegetation acts to increase flow depths, potentially increasing the risk of flooding (Darby, 1999). In stormwater ponds, the resistance of vegetation has a dominant impact on the flow field and therefore affects treatment potential (Sonnenwald, Guymer, & Stovin, 2017). Determining vegetation drag is therefore of interest for a range of hydraulic engineering applications.

1.1 Existing measurements of C_D

Arrays of rigid cylinders are often used to represent emergent vegetation, e.g. Bennett, Pirim, and Barkdoll (2002), Nepf (1999), Rameshwaran and Shiono (2007), Rowiński and Kubrak (2002), Serra, Fernando, and Rodríguez (2004),

Tanino and Nepf (2008b) and Tinoco and Cowen (2013). Table 1 presents seven datasets where the bulk drag coefficient, C_D , for emergent cylinder arrays has been experimentally or numerically derived. The experimental and numerical methods used for determining C_D are described below.

Traditionally, C_D is obtained from experimental results for emergent cylinder arrays by equating driving forces with resistance caused by cylinders (Ferreira, Ricardo, & Franca, 2009; Kim & Stoesser, 2011; Tanino & Nepf, 2008a). Assuming wall and bed stresses are negligible, for emergent cylinders this equates to the balance of gravity and drag forces:

$$\rho g S (1 - \phi) = \frac{1}{2} C_D a \rho U_p^2 \quad (1)$$

where ρ is density, g is acceleration due to gravity, S is channel or energy slope, ϕ is solid volume fraction, a is frontal facing area (the cylinder area perpendicular to the direction

Received 15 June 2017; accepted 19 June 2018/Currently open for discussion.

Table 1 Summary of experimental data describing drag in arrays of emergent cylinders

Study	Distribution	ϕ (–)	d (mm)	R_d (–)	Method
Ferreira et al. (2009)	Random	0.022–0.04	10	1185–1452	Equation (1)
Kim and Stoesser (2011)	Staggered	0.022–0.087	10	761–1738	Equation (1)
Tanino and Nepf (2008a)	Random	0.091–0.35	6.4	24–507	Equation (1)
Tinoco and Cowen (2013)	Random	0.005–0.08	3–25	55–3838	Direct force measurement
Meftah and Mossa (2013)	Square	0.003	3	234–607	Equation (2)
Koch and Ladd (1997)	Random	0.05–0.4	^a	12–99	2D CFD (LBM ^b)
Stoesser et al. (2010)	Staggered	0.015–0.251	6.4	133–1789	3D CFD (LES ^c)

^aNo diameters available.^bLattice Boltzmann method.^cLarge eddy simulation.

of flow per unit volume, $m^2 m^{-3}$), and U_p is mean interstitial velocity (Stone & Shen, 2002; Tanino, 2012). For cylinders $\phi = ad\pi/4$ where d is cylinder diameter. In low velocities or low cylinder densities Eq. (1) is impractical to apply, as it becomes difficult to measure surface slope. Bed and free surface stresses also become more important, eventually invalidating Eq. (1) (Tanino & Nepf, 2008a). Instead, drag may be measured directly using a force sensor (Dittrich, Aberle, Schoneboom, Rodi, & Uhlmann, 2012; James, Goldbeck, Patini, & Jordanova, 2008; Tinoco & Cowen, 2013). Measured force is then equated directly with the the right hand side of Eq. (1).

As an alternative to direct measurement, Nepf (1999) assumed that turbulence production in vegetation (arrays of cylinders) is equal to dissipation, that drag dominates energy dissipation, and therefore that turbulence intensity can be equated to drag force as:

$$\frac{\sqrt{k}}{U_p} = \gamma \left(\frac{1}{(1-\phi)} C_D a d \right)^{1/3} \quad (2)$$

where k is turbulent kinetic energy and $\gamma \approx 1$ (Tanino & Nepf, 2008b). Thus, instantaneous velocity measurements, e.g. from acoustic Doppler velocimetry, may be used to determine k and hence C_D (Meftah & Mossa, 2013).

For simple geometries, such as a single cylinder or periodic arrays of cylinders, C_D may be evaluated using computational fluid dynamics (CFD) tools (Kim & Stoesser, 2011; Koch & Ladd, 1997; Marjoribanks, Hardy, Lane, & Parsons, 2014; Rahman, Karim, & Alim, 2007; Stoesser, Kim, & Diplas, 2010), either by determining S in Eq. (1) from the streamwise pressure gradient or by extracting the force on a cylinder by integrating the pressure acting on the cylinder wall.

1.2 C_D estimation functions

When no physical measurements are available and CFD-based approaches are infeasible (e.g. a complex geometry) C_D must be estimated. It is well established that C_D for a single-cylinder is dependent on cylinder Reynolds number R_d , where $R_d = U_p d \nu^{-1}$ and ν is kinematic viscosity (Schlichting, Gersten, Krause, Oertel, & Mayes, 1960; White, 1991). For

cylinder arrays, C_D is also dependent on array characteristics (Nepf, 1999). Table 2 lists several functions that estimate C_D depending on array (or vegetation) characteristics. These functions all have a basis in experimental observations and it is of interest to evaluate how successfully they estimate C_D . The White (1991) function is included as a base comparison.

The Tanino and Nepf (2008a) and Tinoco and Cowen (2013) functions share a common derivation. Koch and Ladd (1997) showed the Ergun (1952) expression for pressure drop in packed columns to successfully predict drag force. Tanino and Nepf (2008a) related this expression to drag coefficient giving:

$$C_D = 2 \left(\frac{\alpha_0}{R_d} + \alpha_1 \right) \quad (3)$$

where α_0 and α_1 are coefficients describing viscous and inertial drag effects respectively. Tanino and Nepf (2008a) and Tinoco and Cowen (2013) used their experimental C_D data to estimate α_0 and α_1 . Linking their values of α_0 and α_1 to the physical characteristics of their cylinder arrays led both to propose linear relationships for predicting α_1 as a function of ϕ . Tanino and Nepf (2008a) noted that α_0 appeared to be independent of cylinder array characteristics and omitted the viscous term from Eq. (3) in their function estimating C_D . Tinoco and Cowen (2013) also excluded the viscous component from their function estimating C_D and suggest it is most suitable at $R_d > 1000$. Therefore, in both functions C_D is solely a function of ϕ .

The similarity of the methods used in the Tanino and Nepf (2008a) and Tinoco and Cowen (2013) studies presents an opportunity to combine their results and create enhanced estimates of C_D from Eq. (3). Sonnenwald, Hart, West, Stovin, and Guymer (2017) re-parametrized α_0 and α_1 in terms of ϕ and d . The objectives of this note are (i) to improve the re-parametrizations of Sonnenwald et al. (2017) by including additional experimental data; (ii) to demonstrate the validity of these re-parametrizations by comparing estimates of C_D made using Eq. (3) to experimental data; and (iii) to compare alternative estimates of C_D with the re-parametrized Eq. (3) and with experimental data.

Table 2 Equations of functions that estimate C_D for arrays of emergent cylinders

Reference	Description
Cheng (2012)	Drag coefficient based on pseudofluid model modification of a single-cylinder function ^a $C_D = \left(11 \left(\frac{R_d}{1 + 80\phi} \right)^{-0.75} + 0.9 \left[1 - \exp \left(-\frac{1000(1 + 80\phi)}{R_d} \right) \right] \right) + 1.2 \left[1 - \exp \left(-\left(\frac{R_d}{4500(1 + 80\phi)} \right)^{0.7} \right) \right] (1 - \phi)$
Ghisalberti and Nepf (2004)	Wake shading numerical model ^b $C_D = \frac{C_{D\text{White}}}{1.16} \{ 1.16 - 9.31(ad) + 38.6(ad)^2 - 59.8(ad)^3 \}$
Tanino and Nepf (2008a)	Fit to cylinder array experimental data using Eq. (3) $C_D = 2(0.46 + 3.8\phi)$
Tinoco and Cowen (2013)	Fit to cylinder array experimental data using Eq. (3) $C_D = 2(0.58 + 6.49\phi)$
White (1991)	Fit to single-cylinder experimental data $C_D = 1 + 10.0R_d^{-2/3}$

^aThe pseudofluid model has an S term, but this is omitted here. For $S \leq 1/100$, differences to estimated C_D value are within $\pm 1\%$.

^b $C_{D\text{White}}$ refers to the White (1991) function.

2 A re-parametrization of the Ergun (1952) coefficients

Figure 1 provides a comparison between values of α_0 and α_1 and the corresponding values of ϕ and d for a range of data. Results from Koch and Ladd (1997) are plotted taking lattice units as mm for comparison purposes.

Figure 1a does not suggest any systematic relationship between α_0 and ϕ , which is consistent with the conclusions of Tanino and Nepf (2008a).

Figure 1b shows a positive correlation between α_0 and d . This is mainly due to the results of Tinoco and Cowen (2013), who varied both ϕ and d . Tanino and Nepf (2008a), who varied only ϕ , did not find a relationship with α_0 . It is therefore reasonable to conclude that the variation in α_0 observed by Tinoco and Cowen (2013) is due to d . The results of Koch and Ladd (1997) show a similar trend. Together they suggest a linear relationship between α_0 and d and as a result the data (excluding that of Koch & Ladd, 1997) presented in Fig. 1b have been fit to a linear function, Eq. (4a), shown in Fig. 1b.

Tanino (2012) suggested that viscous drag, the component described by α_0 , is proportional to d/s , where s is cylinder spacing. A linear relationship with d is consistent with this. No relationship between α_0 and s (either on its own or with d) was found.

Figure 1c shows a positive correlation between α_1 and ϕ , which is consistent with both Tanino and Nepf (2008a) and Tinoco and Cowen (2013) who both suggested a linear relationship between α_1 and ϕ . Tanino (2012) suggested that the inertial drag (described by α_1) is strongly linked to flow-field heterogeneity, and that ϕ provides a reasonable estimate of this. Figure 1d also shows a positive correlation between α_1 and d . A linear relationship between α_1 and d is suggested by the results of Tinoco and Cowen (2013) and Koch and Ladd (1997), similar to α_0 . If α_1 also depends on d , then d may serve to indicate flow-field heterogeneity.

Together, Figs 1c and 1d suggest that α_1 is a function of both ϕ and d and all data shown in these two figures (excluding that of Koch & Ladd, 1997) have been used to fit a single function (not shown in Fig. 1). Combining these two parameters gives a

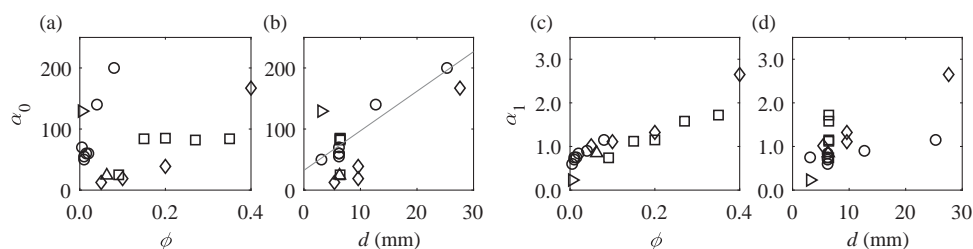


Figure 1 Plots of the Ergun (1952) coefficients with respect to cylinder array characteristics, (a) α_0 vs ϕ , (b) α_0 vs d , (c) α_1 vs ϕ , (d) α_1 vs d ; \blacklozenge Meftah and Mossa (2013), \blacktriangle Stoesser et al. (2010), \square Tanino and Nepf (2008a), \circ Tinoco and Cowen (2013), — best-fit Eq. (4a), \diamond Koch and Ladd (1997) taking lattice units as mm

variation in values of α_1 for the same d . Least-squares curve-fitting was undertaken assuming $\alpha_0 = f(d)$ and $\alpha_1 = f(d, \phi)$ are linear functions giving:

$$\alpha_0 = 6475d + 32 \quad (4a)$$

$$\alpha_1 = 17d + 3.2\phi + 0.50 \quad (4b)$$

where Eq. (4a) provides an estimate of the viscous effects and Eq. (4b) provides an estimate of the inertial effects of drag when used in Eq. (3). Note that the coefficients to the d terms must have units m^{-1} to retain non-dimensionality. Root mean square error (RMSE) values of 38.0 and 0.131 were obtained respectively for α_0 and α_1 . Substituting Eq. (4) into Eq. (3) gives a

new function for estimating C_D :

$$C_D = 2 \left(\frac{6475d + 32}{R_d} + 17d + 3.2\phi + 0.50 \right) \quad (5)$$

3 A comparison of estimates of C_D against experimental results

Figure 2 shows estimates of C_D from the functions in Table 2 and Eq. (5) plotted for a range of R_d , a representative selection of ϕ and d , and with the experimental data from Table 1. Each sub-figure shows increasing ϕ . Most functions show the expected dependency of C_D on R_d except the Tanino and Nepf (2008a) and Tinoco and Cowen (2013) functions, which exclude a viscous term and are therefore poor estimators

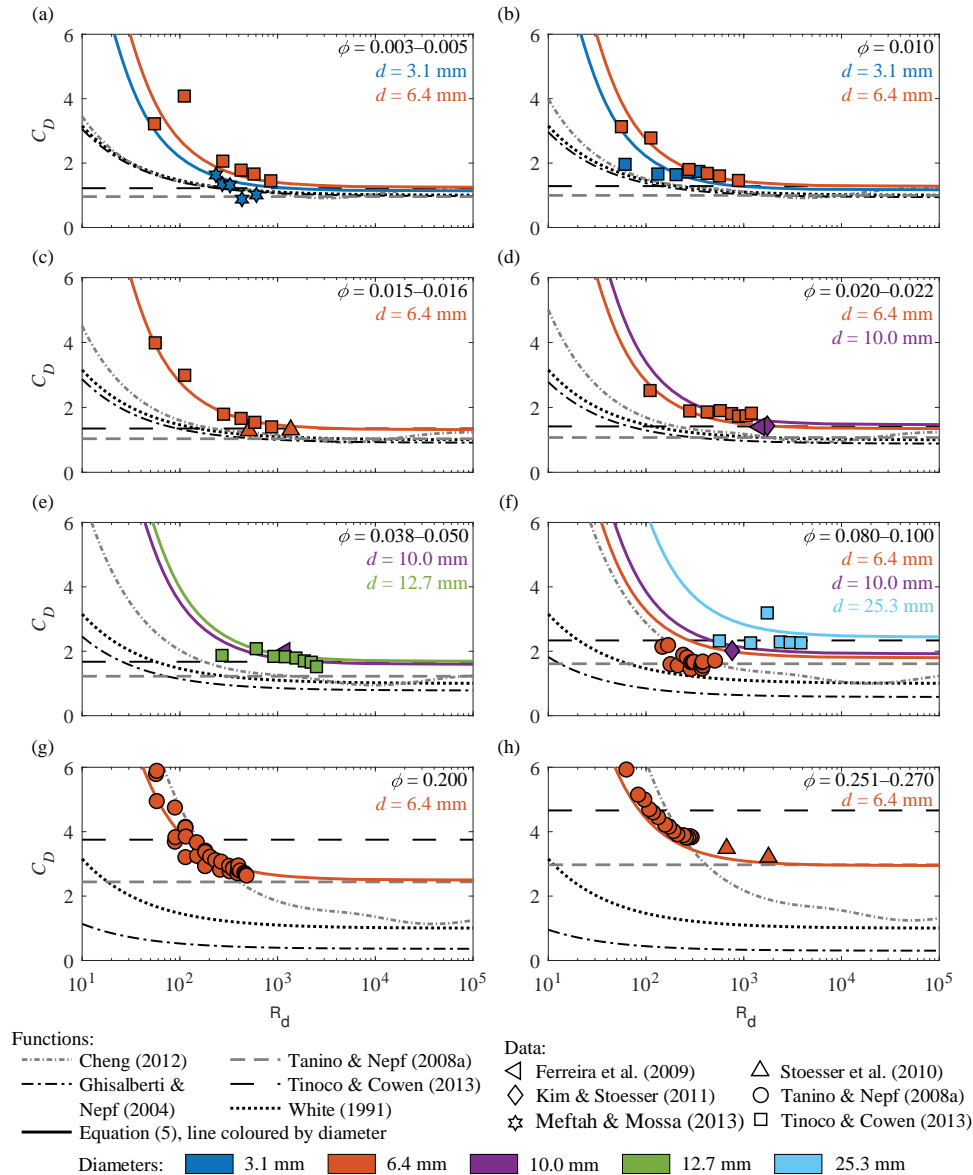


Figure 2 Comparison of experimental values of C_D (data) to estimates (functions) at a selection of different values of ϕ and d (shown in top right corner of plot)

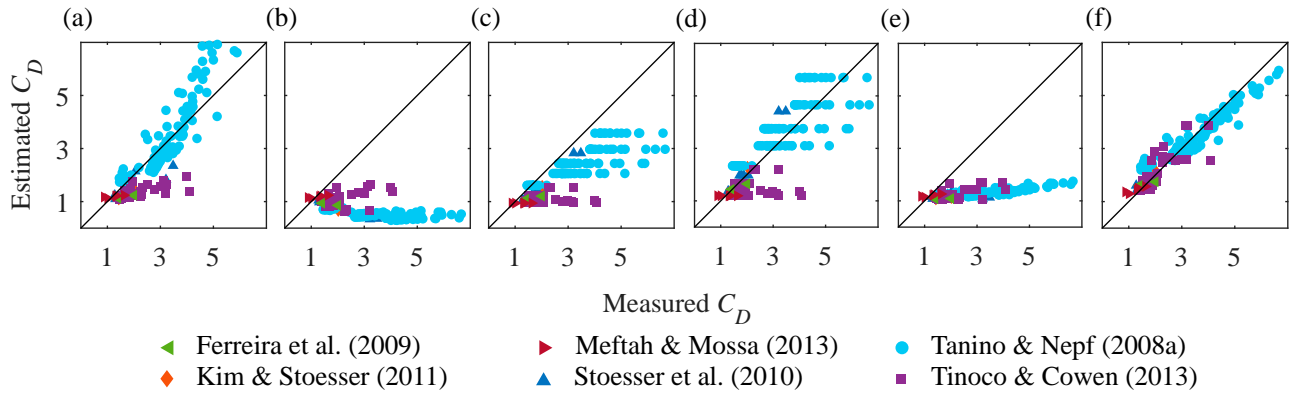


Figure 3 Measured C_D compared with estimated C_D using the functions of (a) Cheng (2012), (b) Ghisalberti and Nepf (2004), (c) Tanino and Nepf (2008a), (d) Tinoco and Cowen (2013), (e) White (1991), and (f) Equation (5); – is a line of equality

of C_D at low R_d . At $\phi \lesssim 0.02$, Fig. 2a–d, most of the functions provide good estimates of C_D for $R_d > 200$, also suggesting that the standard $C_D \approx 1$ is not unreasonable in this range. At $\phi \lesssim 0.01$ and $R_d < 200$, Fig. 2a and 2b, the White (1991), Ghisalberti and Nepf (2004), and Cheng (2012) functions produce similar underestimates of C_D . All three are based on single-cylinder formulations of drag. Figure 2a–d show that only Eq. (5) estimates C_D well at $R_d < 200$.

As ϕ increases, $\phi \gtrsim 0.04$ in Fig. 2e–h, the differences between the C_D values estimated by each function become greater. The White (1991) and Ghisalberti and Nepf (2004) functions consistently underestimate C_D . The Ghisalberti and Nepf (2004) function predicts decreasing C_D with increasing ϕ , which is unique among the functions presented here. The Cheng (2012) function, in contrast, fits the data reasonably well at higher ϕ .

The differences between the Tanino and Nepf (2008a) and Tinoco and Cowen (2013) functions become more apparent at higher ϕ , with the latter estimating greater values of C_D . Compared to the experimental results, the Tinoco and Cowen (2013) function performs better at lower values of R_d (Fig. 2g) while the Tanino and Nepf (2008a) function performs better at higher values (Fig. 2h). Despite their suggestion otherwise, the Tinoco and Cowen (2013) function performs well at $R_d < 1000$. The estimates of C_D made with Eq. (5) fit the data well at higher values of ϕ .

There are several instances where experimental configurations from the studies in Table 1 overlap such that measurements of C_D were taken at the same ϕ but at different d . Figure 2a, 2b, and 2f show that across multiple R_d , C_D increases with d . Equation (5) reproduces this trend, justifying the dependence of Eq. (5) on d . It is the only function that consistently fits the experimental data in Fig. 2.

Figure 3 provides a direct comparison between measured and estimated C_D for each function. The Ghisalberti and Nepf (2004) and White (1991) functions (Fig. 3b and 3e) consistently underestimate C_D with RMSE values of 3.09 and 2.40. The Tanino and Nepf (2008a) function (Fig. 3c)

performs better with an RMSE value of 1.66. The Tinoco and Cowen (2013) function (Fig. 3d) appears to perform well with an RMSE value of 1.16, but shows significant scatter. Horizontal bands in Fig. 3c and 3d indicate that the same C_D value is estimated at the same ϕ despite different values of d and R_d . The Cheng (2012) function (Fig. 3a) also appears to estimate C_D reasonably well, with an RMSE value of 1.28 as it performs less well at higher C_D and ϕ .

Equation (5) (Fig. 3f) has the tightest clustering around the line of equality with an RMSE value of 0.52, showing that of the six functions evaluated it estimates values of C_D closest to experimental measurements. Therefore, the dependence of α_0 and α_1 on ϕ and d suggested by Sonnenwald et al. (2017) is reasonable. Note that these functions have only been tested over the range of $0.003 \leq \phi \leq 0.4$, $0.003 \leq d \leq 0.025$, and $12 \leq R_d \leq 3838$ and care must be taken applying them outside of this range.

4 Conclusions

A re-parametrization of the Ergun-derived coefficients α_0 and α_1 has been presented. This resulted in a function for estimating drag coefficient (C_D), which has been compared to experimental data alongside several other functions estimating C_D in arrays of rigid cylinders representing emergent vegetation. All functions perform well for low solid volume fractions (ϕ) and high cylinder Reynolds number (R_d), and generally the standard $C_D \approx 1$ is not unreasonable here. As R_d decreases, only those functions that include viscous drag effects provide reasonable results. As ϕ increases, many of the functions underestimate C_D . The function detailed in this study, which includes viscous effects, ϕ , and also a dependency on cylinder diameter (d), provides improved estimates of C_D .

Acknowledgments

The authors thank the anonymous reviewers for their feedback.

Funding

This research was funded by the Engineering and Physical Sciences Research Council (EPSRC) [grants EP/K024442/1, EP/K025589/1 and via the Warwick Impact Acceleration Account EP/K503848/1].

Notations

a	= frontal facing area ($\text{m}^2 \text{m}^{-3}$)
C_D	= drag coefficient (–)
d	= cylinder diameter (m)
g	= gravity acceleration (m s^{-2})
k	= turbulent kinetic energy ($\text{m}^2 \text{s}^{-2}$)
R_d	= cylinder Reynolds number (–)
S	= channel slope (–)
s	= cylinder spacing (m)
U_p	= mean interstitial velocity (m s^{-1})
α_0	= coefficient describing viscous effects (m^{-1})
α_1	= coefficient describing inertial effects (–)
γ	= turbulence intensity scaling coefficient (–)
ν	= kinematic viscosity ($\text{m}^2 \text{s}^{-1}$)
ρ	= density (kg m^{-3})
ϕ	= solid volume fraction (–)

ORCID

Fred Sonnenwald  <http://orcid.org/0000-0002-2822-0406>

Virginia Stovin  <http://orcid.org/0000-0001-9444-5251>

Ian Guymer  <http://orcid.org/0000-0002-1425-5093>

References

- Bennett, S. J., Pirim, T., & Barkdoll, B. D. (2002). Using simulated emergent vegetation to alter stream flow direction within a straight experimental channel. *Geomorphology*, 44(1), 115–126.
- Cheng, N. S. (2012). Calculation of drag coefficient for arrays of emergent circular cylinders with pseudofluid model. *Journal of Hydraulic Engineering*, 139(6), 602–611.
- Darby, S. E. (1999). Effect of riparian vegetation on flow resistance and flood potential. *Journal of Hydraulic Engineering*, 125(5), 443–454.
- Dittrich, A., Aberle, J., Schoneboom, T., Rodi, W., & Uhlmann, M. (2012). Drag forces and flow resistance of flexible riparian vegetation. In W. Rodi & M. Uhlmann (Eds.), *Environmental fluid mechanics: Memorial colloquium on environmental fluid mechanics in honour of Professor Gerhard H. Jirka* (pp. 195–215). London: CRC Press, Taylor & Francis Group.
- Ergun, S. (1952). Fluid flow through packed columns. *Chemical Engineering Progress*, 48, 89–94.
- Ferreira, R. M. L., Ricardo, A. M., & Franca, M. J. (2009). Discussion of “Laboratory investigation of mean drag in a random array of rigid, emergent cylinders” by Yukie Tanino and Heidi M. Nepf. *Journal of Hydraulic Engineering*, 135(8), 690–693.
- Ghisalberti, M., & Nepf, H. M. (2004). The limited growth of vegetated shear layers. *Water Resources Research*, 40(7), W07502.
- James, C. S., Goldbeck, U. K., Patini, A., & Jordanova, A. A. (2008). Influence of foliage on flow resistance of emergent vegetation. *Journal of Hydraulic Research*, 46(4), 536–542.
- Kim, S. J., & Stoesser, T. (2011). Closure modeling and direct simulation of vegetation drag in flow through emergent vegetation. *Water Resources Research*, 47(10), W10511.
- Koch, D. L., & Ladd, A. J. C. (1997). Moderate Reynolds number flows through periodic and random arrays of aligned cylinders. *Journal of Fluid Mechanics*, 349, 31–66.
- Marjoribanks, T., Hardy, R., Lane, S., & Parsons, D. (2014). Dynamic drag modeling of submerged aquatic vegetation canopy flows. In A. J. Schleiss, G. de Ceseare, M. J. Franca, & M. Pfister (Eds.), *River Flow 2014* (pp. 517–524). London: CRC Press, Taylor & Francis Group.
- Meftah, M. B., & Mossa, M. (2013). Prediction of channel flow characteristics through square arrays of emergent cylinders. *Physics of Fluids*, 25(4), 045102.
- Nepf, H. M. (1999). Drag, turbulence, and diffusion in flow through emergent vegetation. *Water Resources Research*, 35(2), 479–489.
- O’Hare, M. T. (2015). Aquatic vegetation—a primer for hydrodynamic specialists. *Journal of Hydraulic Research*, 53(6), 687–698.
- Rahman, M. M., Karim, M. M., & Alim, M. A. (2007). Numerical investigation of unsteady flow past a circular cylinder using 2-D finite volume method. *Journal of Naval Architecture and Marine Engineering*, 4(1), 27–42.
- Rameshwaran, P., & Shiono, K. (2007). Quasi two-dimensional model for straight overbank flows through emergent vegetation on floodplains. *Journal of Hydraulic Research*, 45(3), 302–315.
- Rowiński, P. M., & Kubrak, J. (2002). A mixing-length model for predicting vertical velocity distribution in flows through emergent vegetation. *Hydrological Sciences Journal*, 47(6), 893–904.
- Schlichting, H., Gersten, K., Krause, E., Oertel, H., & Mayes, K. (1960). *Boundary-layer theory* (Vol. 7). Berlin: Springer.
- Serra, T., Fernando, H. J. S., & Rodríguez, R. V. (2004). Effects of emergent vegetation on lateral diffusion in wetlands. *Water Research*, 38(1), 139–147.
- Sonnenwald, F., Guymer, I., & Stovin, V. (2017). Computational fluid dynamics modelling of residence times in vegetated stormwater ponds. *Proceedings of the Institution of Civil Engineers - Water Management*, 171(2), 76–86.

- Sonnenwald, F., Hart, J. R., West, P., Stovin, V. R., & Guymer, I. (2017). Transverse and longitudinal mixing in real emergent vegetation at low velocities. *Water Resources Research*, 53(1), 961–978.
- Stoesser, T., Kim, S. J., & Diplas, P. (2010). Turbulent flow through idealized emergent vegetation. *Journal of Hydraulic Engineering*, 136(12), 1003–1017.
- Stone, B. M., & Shen, H. T. (2002). Hydraulic resistance of flow in channels with cylindrical roughness. *Journal of hydraulic engineering*, 128(5), 500–506.
- Tanino, Y. (2012). Flow and mass transport in vegetated surface waters. In C. Gualtieri & D. T. Mihailovic (Eds.), *Fluid mechanics of environmental interfaces* (2nd ed., pp. 369–394). Abingdon: Taylor & Francis.
- Tanino, Y., & Nepf, H. M. (2008a). Laboratory investigation of mean drag in a random array of rigid, emergent cylinders. *Journal of Hydraulic Engineering*, 134(1), 34–41.
- Tanino, Y., & Nepf, H. M. (2008b). Lateral dispersion in random cylinder arrays at high Reynolds number. *Journal of Fluid Mechanics*, 600, 339–371.
- Tinoco, R. O., & Cowen, E. A. (2013). The direct and indirect measurement of boundary stress and drag on individual and complex arrays of elements. *Experiments in Fluids*, 54(4), 1–16.
- White, F. M. (1991). *Viscous fluid flow*. New York: McGraw-Hill.